MOLECULAR
METABOLISM

The neuropeptide TLQP-21 opposes obesity via C3aR1-mediated enhancement of adrenergic-induced lipolysis

CrossMark

Cheryl Cero [1], Maria Razzoli [1], Ruijun Han [1], Bhavani Shankar Sahu [1], Jessica Patricelli [1], ZengKui Guo [3], Nathan A. Zaidman [1], John M. Miles [3], Scott M. O'Grady [2], Alessandro Bartolomucci [1],*

ABSTRACT

Objectives: Obesity is characterized by excessive fat mass and is associated with serious diseases such as type 2 diabetes. Targeting excess fat mass by sustained lipolysis has been a major challenge for anti-obesity therapies due to unwanted side effects. TLQP-21, a neuropeptide encoded by the pro-peptide VGF (non-acronymic), that binds the complement 3a receptor 1 (C3aR1) on the adipocyte membrane, is emerging as a novel modulator of adipocyte functions and a potential target for obesity-associated diseases. The molecular mechanism is still largely uncharacterized.

Methods: We used a combination of pharmacological and genetic gain and loss of function approaches. 3T3-L1 and mature murine adipocytes were used for *in vitro* experiments. Chronic *in vivo* experiments were conducted on diet-induced obese wild type, β_1, β_2, β_3-adrenergic receptor (AR) deficient and C3aR1 knockout mice. Acute *in vivo* lipolysis experiments were conducted on Sprague Dawley rats.

Results: We demonstrated that TLQP-21 does not possess lipolytic properties *per se*. Rather, it enhances β-AR activation-induced lipolysis by a mechanism requiring Ca^{2+} mobilization and ERK activation of Hormone Sensitive Lipase (HSL). TLQP-21 acutely potentiated isoproterenol-induced lipolysis *in vivo*. Finally, chronic peripheral TLQP-21 treatment decreases body weight and fat mass in diet induced obese mice by a mechanism involving β-adrenergic and C3a receptor activation without associated adverse metabolic effects.

Conclusions: In conclusion, our data identify an alternative pathway modulating lipolysis that could be targeted to diminish fat mass in obesity without the side effects typically observed when using potent pro-lipolytic molecules.

1. INTRODUCTION

Obesity is a disease characterized by excessive white adipose tissue (WAT) accumulation caused by an imbalance between input and expenditure of energy over time [1,2]. Excess adiposity is associated with several chronic diseases [3,4] and also compromises the normal physiological regulation of adipogenesis/lipolysis leading to the so-called lipolytic catecholamine resistance in adipocytes [5–7]. Lipolysis, the hydrolysis of triacylglycerol (TAG) into non-esterified free fatty acids (FFA) and glycerol, has a central role in lipid storage and energy homeostasis. Preventing fat accumulation and fine-tuning lipid breakdown are key to normalizing obesity and its comorbidities. However, the pharmacological exploitation of lipolytic processes as an anti-obesity strategy has so far been hindered by metabolic and cardiovascular side effects exerted by potent pro-lipolytic molecules such as norepinephrine (NE), sympathomimetics, as well as peptides eliciting increased intracellular cAMP or cGMP levels [8–11]. Thus, identifying alternative, safer pathways to increase lipolysis would be of

major translational relevance. Specifically, molecules that are *per se* not pro-lipolytic but that act as downstream enhancers/sensitizers of endogenous adrenergic-stimulation of lipolysis have the potential to decrease fat mass without causing an overshoot of circulating free fatty acids and associated insulin resistance.

Here we identified a novel lipolytic and anti-obesity mechanism exerted by TLQP-21, a neuropeptide encoded by the pro-peptide VGF (non-acronymic), that targets primarily the complement 3a receptor 1 (C3aR1) on the adipocyte membrane [12–15]. TLQP-21 is expressed in the central nervous system and peripheral nervous system, including sympathetic nerve terminal in the adipose tissue [12,13,16]. Intracerebroventricular infusion of TLQP-21 in mice prevents the onset of obesity by increasing energy expenditure [12]. Furthermore, TLQP-21 modulates adrenergic-induced lipolysis and increases sympathetic innervation to the fat pads [13], attenuates the development of type 2 diabetes via enhancement of islet β-cell survival and function [17], and normalizes obesity-induced hypertension [18]. Importantly, obese mice are characterized by low expression of VGF C-terminal peptides,

[1]Department of Integrative Biology and Physiology, University of Minnesota, 2231 6th St. SE, Minneapolis, MN 55455, USA [2]Department of Animal Science, Integrative Biology and Physiology, University of Minnesota, 480 Haecker Hall, 1364 Eckles Avenue, St Paul, MN 55108, USA [3]Endocrine Research Unit, Division of Endocrinology, Diabetes, Metabolism and Nutrition, Department of Internal Medicine, Mayo Foundation, 5-194 Joseph, Rochester, MN 55905, USA

*Corresponding author. E-mail: abartolo@umn.edu (A. Bartolomucci).

148 MOLECULAR METABOLISM 6 (2017) 148–158 www.molecularmetabolism.com

including TLQP-21 [19], and by increased expression of C3aR1 [13,20], overall suggesting that the altered TLQP-21/C3aR1 pathway is functionally associated with obesity. However, the molecular mechanism is still largely uncharacterized.

In this study, we showed that TLQP-21 does not possess lipolytic properties *per se*. Rather, it enhances β-adrenergic receptor (β-AR) activation-induced lipolysis by a mechanism requiring Ca^{2+} mobilization and ERK activation of Hormone Sensitive Lipase (HSL). Furthermore, chronic peripheral TLQP-21 treatment can decrease body weight and fat mass in diet induced obese mice by a mechanism requiring C3aR1 receptor and concomitant β-AR receptor activation without the adverse metabolic effects normally associated with the use of adrenergic receptor agonists. These results identify a novel calcium-mediated mechanism for the control of lipolysis and, in the context of a previously established safe cardiovascular profile [12,18], establish TLQP-21/C3aR1 as a novel promising target for anti-obesity therapies.

2. METHODS

2.1. Experimental animals
β1,β2,β3-AR deficient (β-less) mice and their respective WT background strain [21], C3aR1 KO and their respective WT background strain, BALBc/J (Jackson Labs), and Sprague Dawley male rats (~400 g; Charles River) were used in the *in vivo* experiments. All protocols were approved by the University of Minnesota or the Mayo Clinic Institutional Animal Care and Use Committees (IACUC).

2.2. Peptides
TLQP-21 and the R21A mutant were synthesized as previously described [14].

2.3. Cell culture
3T3-L1 cells (from Molecular and Cellular Basis of Obesity Core, Minnesota Obesity Center) were plated on 6-well plates and maintained in DMEM with supplemented with 10% fetal calf serum (FCS) (Lonza) and with 100 units/ml of penicillin/streptomycin (Invitrogen, Carlsbad, CA) in a humidified atmosphere of 5% CO_2 at 37 °C. Media was changed every other day until cells were confluent. Once confluent, differentiation into adipocytes was initiated by using a differentiation cocktail containing 10% fetal bovine serum (FBS) (Atlas) 0.5 mM methylisobutylxanthine (Sigma Aldrich, Saint Louis, MO), 10 μg/ml insulin (Sigma Aldrich, Saint Louis, MO), and 0.25 μM dexamethasone (Sigma Aldrich, Saint Louis, MO). After 48 h, the media was replaced with FBS medium supplemented only with 10 μg/ml insulin, which was removed after 2 days. Thereafter, the differentiated cells were maintained in DMEM with 10% FBS and media changed every other day until used in experiments 8—9 days after induction. Perigonadal white adipose tissue (pWAT) from WT and β-less mice was dissected under sterile conditions and washed in KRH buffer + 1% BSA fatty acid free (Roche). After finely mincing and digesting the tissue using collagenase type II (Sigma) for 30 min at 37 °C in KRH buffer + 1%BSA, the digestion was then stopped by adding KRH + 1% BSA and the cell suspension centrifuged at 200 g for 3 min to separate mature single adipocytes from the stromal vascular fraction. The adipocyte cell suspension was extensively washed and passed through a 100 μM cell strainer to separate single cells. A similar protocol was used for the isolation of pre-adipocytes, where HBSS was used instead of KRH for the isolation process. The cell suspension was filtered through a 25 μM mesh to remove endothelial cells. Isolated stroma vascular cells were plated onto 12-well plates in DMEM/F12 + 10%FCS at a density of

150,000 cells/cm². Once confluency was reached, differentiation was induced by the addition of induction media containing 250 μM methylisobutylxanthine (Sigma Aldrich, Saint Louis, MO), 10 μg/ml insulin (Sigma Aldrich, Saint Louis, MO), 100 nM dexamethasone (Sigma Aldrich, Saint Louis, MO), and 60 μM of indomethacin. After 48 h, the induction media was replaced with insulin containing media, which was removed after 2 days. From that day forward, the maintenance media, DMEM/F12 + 10% FBS, was replaced every other day, and differentiated cells were used at day 8—9 after induction.

2.4. Lipolysis experiments *in vitro*
3T3-L1 adipocytes were serum-starved in Krebs—Ringer buffer containing HEPES (KRH buffer) (NaCl at 120 mM; KCl at 4.7 mM; $CaCl_2$ at 2.2 mM; HEPES at 10 mM; KH_2PO_4 at 1.2 mM; $MgSO_4$ at 1.2 mM; glucose at 5.4 mM) supplemented with 1% bovine serum albumin (BSA) fatty acid free (Roche) for 3 h. Following starvation, the cells were incubated with KRH buffer containing 4% BSA with TLQP-21 or C3a (10 nM — 1 μM) in the presence and absence of isoproterenol (ISO) (Sigma) at concentrations ranging from 1 nM to 1 μM or forskolin (100 nM—10 μM) (Sigma). For the Ca^{2+} mobilization experiments, intracellular chelator 1,2-bis (*o*-aminophenoxy)ethane-*N*,*N*,*N'*,*N'*-tetraacetic acid tetra (acetoxy-methyl) ester (BAPTA-AM) (Sigma) and/or ethylene glycol tetraacetic acid (EGTA) (1 mM) was used. Briefly, 3T3-L1 differentiated cells were pre-exposed to 5 μM BAPTA-AM for 10 min in KRK-4% BSA, then removed and replaced with buffer containing 100 nM ISO and 100 nM TLQP-21 treatments or the combination of both treatments. 1 mM EGTA was added along with 100 nM ISO, 100 nM TLQP-21 or both treatments for 3 h. Lipolysis with U0126 (Calbiochem) was performed on cells pretreated with 1 μM U0126 for 1 h, then exposed to ISO and TLQP-21. All 3T3-L1 cells lipolysis measurements were made over a 3 h period at 37 °C and 5% CO_2.

In the WT and β-less primary adipocytes' lipolytic experiments, 150—200,000 adipocytes were incubated in KRH buffer + 4% BSA with ISO (1 nM, 10 nm, 100 nM, 1 μM, 10 μM) or Forskolin (10 μM) for 180 min at 37 °C with constant shaking at 140 rpm.

In all experiments, lipolysis was measured as the rate of glycerol release into the induction media. Following the incubation period, the media was collected, placed on ice for 10 min, and then placed in a water bath at 60 °C for 20 min to inactivate any residual enzymatic activity. The induction media was then stored at −20 °C until the glycerol assay was performed. Glycerol concentration in the conditioned media was measured using the Free Glycerol Determination kit (Sigma) in a flat-bottom 96-well plate following the manufacturer's instructions All samples were allowed to incubate for 15 min at room temperature prior to measuring the absorbance at 540 OD on a plate reader (Synergy H1, BioTEK). Glycerol content was normalized to total cellular protein content determined by Bradford Assay (Thermo Scientific). The data were normalized to the control response detected in the same experiment and expressed as fold change over controls.

2.5. mRNA extration, reverse transcription and quantitative real-time PCR
RNA was obtained by homogenizing around 50—100 mg of frozen tissue in 500 ml of TRI REAGENT (Molecular Research Center, Inc., Cincinnati, Ohio) on ice following manufacturer's instructions. Total RNA was digested with Dnase I using DNA-free (Ambion, Austin, TX) and tested for the presence of DNA contamination using PCR. Total RNA concentration and purity was then determined by spectrophotometer at 260 nm (NanoDrop 2000 UV—Vis Spectrophotometer, Thermo Scientific). 500 ng of RNA was converted into cDNA using

iScript cDNA Synthesis Kit (Bio-Rad Laboratories, Hercules, CA) and relative quantification of mRNAs was performed with 3.5 μl of cDNA used in each 11.5 μl real-time-RT-PCR reaction using C1000 thermal cycler™ (Bio-Rad Laboratories, Hercules, CA). The PCR reactions were carried out using IQ™ Syber Green Supermix (BIO-RAD). Primers for the target genes are presented in Table S1. Thermal cycling parameters were as follows: an initial denaturing step (95 °C for 10 min), followed by 40 cycles of denaturing, annealing, and extending (95 °C for 45 s, 58 °C for 45 s and then 60 °C for 1 min, respectively) in a 96-well BioRad plate. The results were calculated by the comparative C_t method using β-actin as an endogenous reference gene, according to the Applied Biosystems ABI PRISM 7700 User Bulletin #2. The expression relative to β-actin was determined by calculating $2^{-\Delta Ct}$.

2.6. Western blot

3T3-L1 adipocytes were rinsed 3X with cold PBS and harvested in RIPA buffer containing protease (Complete Mini, Roche) and phosphates inhibitors (Thermo Scientific). Cells were incubated for 10 min [13] with ISO (50 nM), TLQP-21 (10 μM) or a combination of the two treatments in presence or absence of pre-incubation for 1 h with U0126 dissolved in DMSO (0.002%) or vehicle alone. Lysates were then sonicated and centrifuged at 12,000 rpm for 10 min to remove nuclei. Protein was determined by BCA assay (Thermo Scientific) and an equivalent concentration of cell lysates were prepared in sodium dodecyl sulfate (SDS) sample buffer and boiled for 5 min at 95 °C. Proteins were resolved by a (4–20%) SDS-polyacrylamide gel electrophoresis (Bio-Rad) and transferred to a PVDF membrane (Bio-Rad) by using a turboblot system from Bio-Rad. Individual proteins were detected with the specific primary antibodies by overnight incubation at 4 °C (tubulin #2146), pHSL (Ser660; #4126), pERK1/2 (Thr202/Tyr204, #9101) all from Cell Signaling at 1:1000 dilution. The HRP conjugated anti-rabbit antibody was used as a secondary antibody at 1:7000 dilutions and the blot was exposed to luminol enhancer solution by using ECL prime reagent (GE health care), further imaged using a chemidoc documentation system from Bio-Rad laboratories.

2.7. *In vivo* peptide treatment experimental procedure

4–6 weeks old male mice were used in these experiments. Before starting the experiments, mice were housed in same-sex groups (3–4 per cage) under standard laboratory conditions at a constant temperature of 22 ± 2 °C in a 12 h light/12 h dark cycle, with chow and water available ad libitum. Mice were fed a 60% kcal high-fat diet (HFD, D12492, – Research Diets, Inc. 5.24 kcal/g) for 9 weeks to induce a diet-induced obesity phenotype that continued for the entire duration of the pharmacological treatment or a standard diet (STD, D12405B, Research Diet, 3.85 kcal/g, 10% kcal from fat). After 9 weeks on HFD, the obese mice were individually housed for baseline recording of body weight, food intake, and body composition. Afterwards, mice were randomized to receive peptide (TLQP-21 [12] or R21A [14] 5 mg/kg/d) or saline daily via i.p. injection (the dose was chosen based on published results [13,17] and a preliminary dose-response experiment (data not shown)). Food intake and body weight were monitored every other day. Whole body composition scanning was performed weekly using the Echo-MRI 3-in-1 (Echo Medical System). Glucose tolerance testing (GTT) was performed on week 3 of treatment. On week 4, whole body energy expenditure was monitored using indirect calorimetry. Mice were decapitated following brief CO_2 anesthesia, and pWAT and subcutaneous (sc) WAT were manually collected, snap frozen and stored at −80 °C. Liver and quadriceps

muscle biopsies were dissected and tissue composition analyzed with the EchoMRI 3-in-1.

2.8. Indirect calorimetry

Oxygen consumption (VO_2) and carbon dioxide production (VCO_2) were measured using the Oxymax Comprehensive Lab Animal Monitoring System (Columbus Instruments). Energy expenditure was calculated with the formula provided by the manufacturer, expressed as kcal/h and analyzed with body weight as continuous predictors in an ANCOVA model [22,23].

2.9. Acute lipolysis *in vivo*

Sprague Dawley male rats (~400 g) were acutely catheterized in a tail artery under local anesthesia for repeated blood collections. Briefly, the rats were restrained in a supine position in a clear plastic cylinder with the tail fully exposed in the lower end. Lidocaine (2%) was injected subcutaneously using an insulin syringe on the ventral side of the tail root. When reflexes in the tail disappeared, a 1 cm-incision was made in the ventral skin 1 inch distal to the injection site at the tail root. The subcutaneous tissues were carefully separated with precision surgical instruments to expose the tail artery. A 22 gauge 1 inch (0.9 × 25 mm) flexible plastic catheter (BD InsyteTM I.V. catheter, BD VialonTM Material, Ref. #381223, Becton Dickinson Infusion Therapy System, Sandy, UT) was then inserted into the artery and secured with sutures to a nearby ligament to prevent accidental pull-out. The skin incision was closed by sutures and covered up using sticky tape with layers of absorbent paper underneath that were saturated with the longacting local anesthetic bupivacaine. The catheterized rats were transferred into a metabolic cage with the entire tail and the catheter exposed to the exterior through a hole in the cage wall. After 30 min of recovery in the cage, an intravenous infusion line was installed in a lateral tail vein instantaneously by transdermal venipuncture. The experiments were conducted in the morning under natural living conditions (i.e., non-fasting). Blood samples were taken at 5–10 min intervals for the measurement of FFA concentrations. ISO infusion (30 ng/min) was then started and continued for 60 min. After 15 min of equilibration, TLQP-21 (40 μg) (n = 8) or saline (n = 8) was injected via the infusion line as a bolus.

2.10. NMR lipidomic

Lipids were extracted from plasma by chloroform:methanol:water extraction with the final solution containing chloroform:methanol (1:2, v/v) and 3,4,5-trichloropyridine as an internal standard. NMR spectra were using a gradient-enhanced 1D NOESY-pre-saturation pulse sequence for water suppression on a Bruker Avance III 700-MHz spectrometer with a TCI 1.7-mm cryoprobe at the Minnesota NMR Center. Acquisition parameters were as follows: 2 s relaxation delay, 4.1 ms mixing time, 4 s acquisition time, 20 ppm sweep width, 8 dummy scans, and 128 transients. 1H 90° pulse width and transmitter offset were optimized for each sample. All spectra were zero-filled to 128 k data points, Fourier transformed with 1 Hz line broadening applied, manually phased, baseline corrected, and integrated using Topspin software [24,25].

2.11. Statistical analysis

Statistical analyses were performed with Statistica 12.0 (Dell Inc.), and significance was set at $p < 0.05$. Data were analyzed with t-test or analysis of variance (ANOVA) followed by Tukey post hoc test. For the *in vitro* experiments, data are reported as the means ± SEM from at least 2–5 independent experiments with n = 3 for each experiment. Sample size for the *in vivo* experiments are provided in the figure legends.

3. RESULTS

3.1. C3aR1 activation is not pro-lipolytic *per se* but enhances β-adrenergic-induced lipolysis in adipocytes

TLQP-21 recently emerged as a neuropeptide modulator of lipolysis and an endogenous ligand for the C3aR1 [13–15]. Consistent with the function of TLQP-21 as an enhancer of β-AR induced lipolysis ([13,14] and Figure 1A) we showed that the C3aR1 agonist $C3a_{70-77}$ [26,27] is not pro-lipolytic *per se* but enhanced lipolysis induced by the non-selective βAR agonist isoproterenol (ISO) in 3T3-L1 adipocytes (Figure 1B, Figure S1A), thus mimicking the effect exerted by TLQP-21. The best characterized pro-lipolytic pathway in adipocytes involves Gs-mediated increase of cAMP and PKA phosphorylation [8]. Previous work demonstrated that TLQP-21 treatment and C3aR1 activation do not increase $[cAMP]_i$ and PKA substrate phosphorylation, yet TLQP-21 robustly enhances βAR-mediated lipolysis [13–15]. To investigate the requirement of βAR signaling for the TLQP-21 pro-lipolytic effect, we compared the lipolytic effect exerted by the peptide in presence of the βAR agonist ISO or the adenylate cyclase (AC) activator forskolin (Forsk). As expected [28,29], ISO and Forsk induced a dose-dependent increase of free glycerol release from 3T3-L1 adipocytes (Figure S1A,C). TLQP-21 enhanced lipolysis induced by both ISO and Forsk (Figure 1A,C), indicating that cAMP mobilization is critical for TLQP-21-induced lipolysis. To further extend our results, we used adipocytes from β_1, β_2, β_3-AR deficient (β-less) mice. β-less adipocytes were unresponsive to ISO treatment but responsive to Forsk, indicating that the lipolytic pathway downstream of β-AR activation is maintained [30] (Figure S1D). Similarly to the effects exerted in 3T3-L1, TLQP-21 potentiated Forsk-induced lipolysis in primary β-less adipocytes (Figure 1D) although with a slightly different pharmacology

compared to 3T3-L1 cells that can be explained by the altered signaling and biogenesis characteristic of this model [21,30].

Overall, our findings demonstrate that βAR and adenylate cyclase activation exert a permissive effect on TLQP-21-induced lipolysis.

3.2. TLQP-21 increases lipolysis via a mechanism dependent upon intracellular Ca^{2+} mobilization and ERK activation

TLQP-21 treatment and C3aR1 activation increase intracellular Ca^{2+} concentration ($[Ca^{2+}]_i$) in several cell types [15,31–35]. Therefore, we hypothesized that TLQP-21-prolipolytic effect is $[Ca^{2+}]_i$-mediated. To provide functional evidence of this mechanism 3T3-L1 adipocytes were pretreated with the intracellular Ca^{2+} chelator BAPTA-AM, a cell-permeable molecule enzymatically converted to the non cell-permeable Ca^{2+} chelator BAPTA once within the cell, and measured lipolysis in presence of ISO with or without TLQP-21. BAPTA-AM had no effect on ISO-induced lipolysis while it abrogated TLQP-21-induced enhancement of ISO-stimulated lipolysis (Figure 2A). Additionally, to determine if TLQP-21 stimulated Ca^{2+} uptake from the extracellular medium, cells were treated with EGTA, an extracellular Ca^{2+} chelating agent. As observed with BAPTA-AM, EGTA pretreatment had no effect on ISO-induced lipolysis while it prevented the TLQP-21-induced enhancement of ISO-stimulated lipolysis (Figure 2B). Overall, our data indicate that Ca^{2+} mobilization involving activation of Ca^{2+} uptake from the extracellular media is required for TLQP-21 enhanced lipolysis. However, we were unable to detect changes in $[Ca^{2+}]_i$ using FURA-AM even after priming the cells with ATP/UTP (data not shown) [15], a result which is consistent with the lack of PLC/PKC phosphorylation induced by TLQP-21 in adipocytes [13].

The role of $[Ca^{2+}]_i$ in adipocyte function is poorly understood. Increased $[Ca^{2+}]_i$ has been shown to modulate lipolysis via the Raf/MAPK/ERK
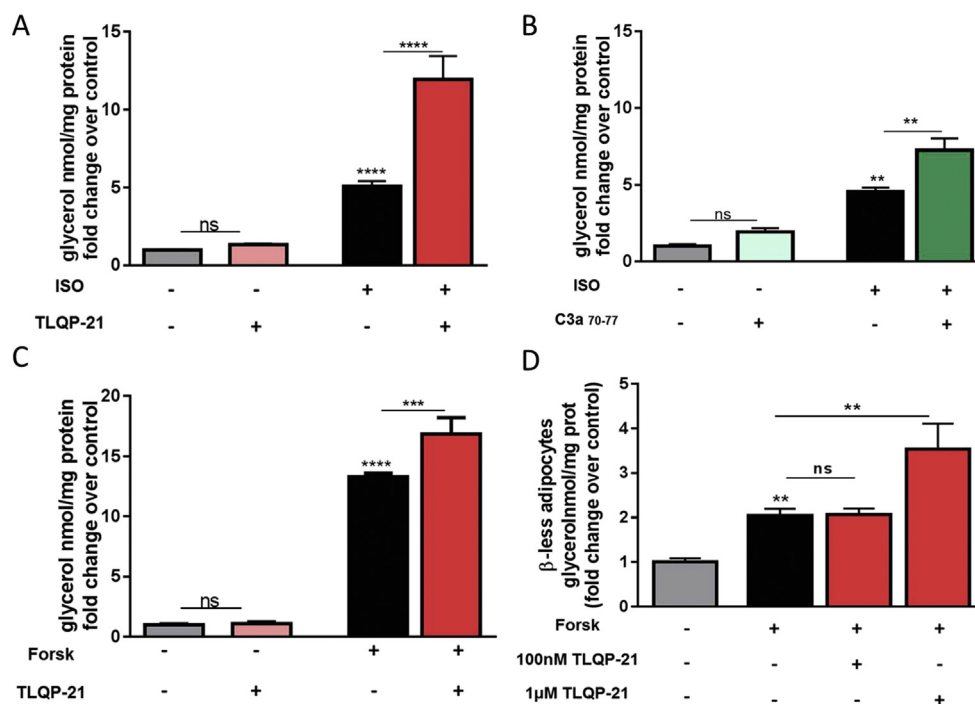
Figure 1: TLQP-21 potentiates isoproterenol and forskolin-induced lipolysis. (A) TLQP-21 potentiates ISO-induced lipolysis in 3T3-L1 adipocytes [F (3,48) = 232.5, p < 0.0001; ISO 50 nM, TLQP-21 100 nM]. (B) $C3a_{70-77}$ potentiates ISO-induced lipolysis in 3T3-L1 adipocytes [F (3,17) = 23.83, p < 0.0001; ISO 50 nM, $C3a_{70-77}$ 100 nM]. (C) TLQP-21 potentiates forskolin (Forsk)-induced lipolysis in 3T3-L1 adipocytes [F (3,17) = 403.5, p < 0.0001; Forsk 10 μM, TLQP-21 100 nM]. (D) TLQP-21 Forsk-induced lipolysis in β-less adipocytes [F (2,8) = 17.82, p = 0.0011; Forsk 10 μM]. *p < 0.001, **p < 0.001, ***p < 0.0001.
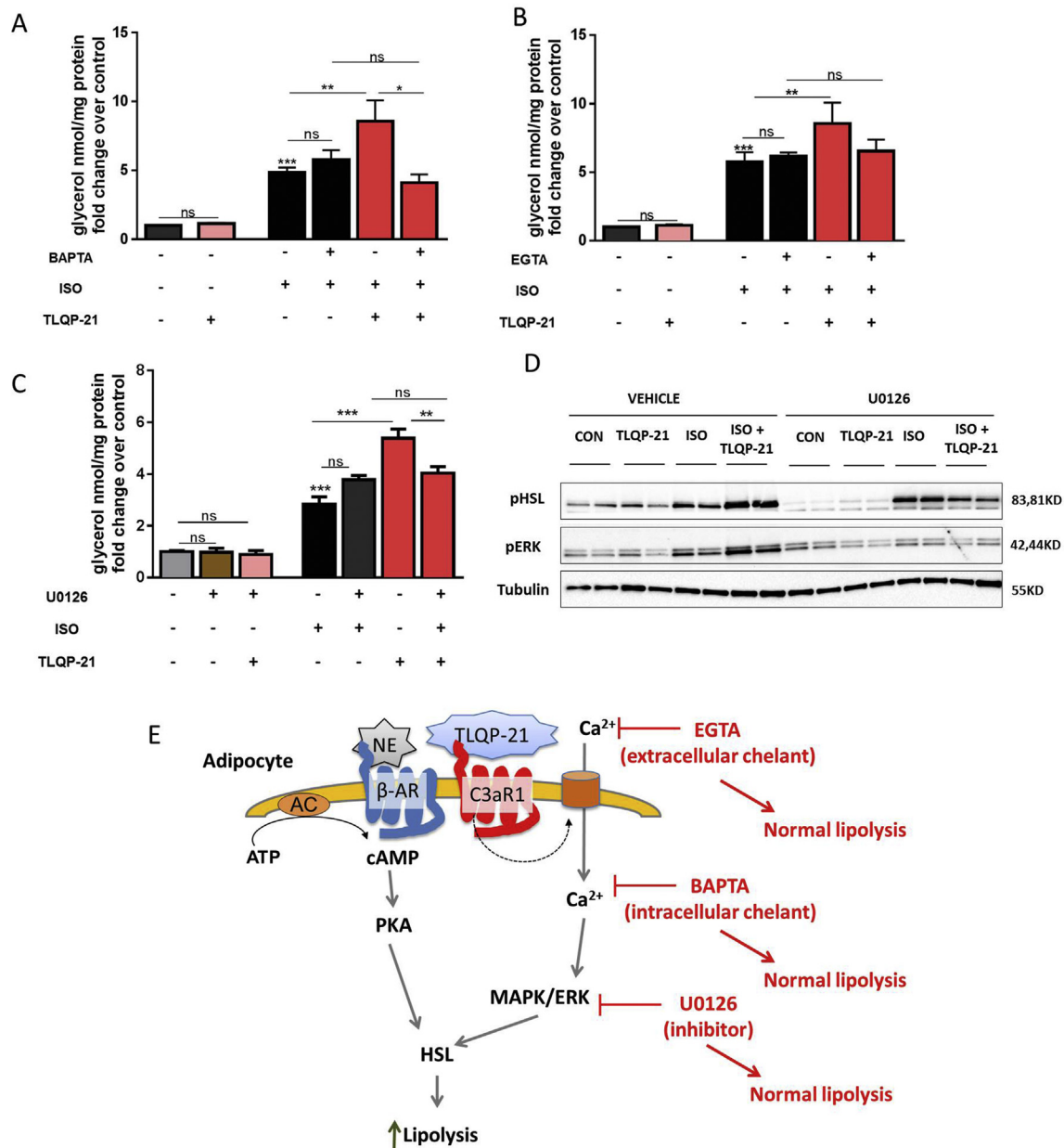
Figure 2: TLQP-21-induced lipolysis requires increased intracellular Ca^{2+} and activation of MAPK/ERK pathway. (A—B) TLQP-21 potentiation of ISO-induced lipolysis is blocked by the intracellular Ca^{2+} chelator BAPTA-AM (5 μM) [F (5,98) = 36.4, p < 0.0001, ISO 100 nM, TLQP-21 100 nM], and the extracellular Ca^{2+} chelator EGTA (1 mM) [F (5,100) = 40.04, p < 0.0001, ISO 100 nM, TLQP-21 100 nM]. (C) Pre-incubation (1hr) with the MAPK/ERK inhibitor U0126 (1 μM) prevents TLQP-21-induced lipolysis [F (6,14) = 96.87, p < 0.0001; ISO 50 nM, TLQP-21 100 nM]. (D). Western blot analysis of ISO and TLQP-21 modulation of pERK and pHSL in presence and absence of U0126 (ISO 50 nM, TLQP-21 10 μM, U0126 1μM). (E) Proposed model of TLQP-21 induced pro-lipolytic effect. ns, non-significant, *p < 0.001, **p < 0.001, ***p < 0.0001.

pathway [36—39], and TLQP-21 enhanced ISO-induced phosphorylation of ERK and HSL [13]. Overall, these findings led us to hypothesize that TLQP-21 activation of C3aR1 could signal via the MAPK/ERK pathway to potentiate ISO-induced lipolysis. Consistent with this hypothesis, pre-treatment with the MAPK inhibitor U0126 completely prevented TLQP-21-induced pro-lipolytic effect without altering ISO-induced lipolysis (Figure 2C). Furthermore, U0126 also abolished TLQP-21 potentiation of ISO-induced ERK and HSL phosphorylation (Figure 2D). Overall, these data demonstrate that TLQP-21-enhancement of β-AR induced lipolysis is mediated by intracellular Ca^{2+} mobilization and ERK activation resulting in enhanced HSL activation (Figure 2E).

3.3. TLQP-21 acutely enhances β-adrenergic receptor-induced lipolysis *in vivo*

Having characterized the TLQP-21 pro-lipolytic mechanism *in vitro*, we tested the acute effect of TLQP-21 on ISO-induced lipolysis *in vivo* using a rat model. Lipolysis more than doubled during continuous ISO-infusion, while it progressively decreased in saline injected rats likely due to tachyphylaxia [40,41]. In contrast, there was no decrease of FFA in the TLQP-21 treated group (Figure 3A). This result is consistent with the *in vitro* data and suggests that TLQP-21 functions as an enhancer of adrenergic receptor-induced lipolysis *in vivo* as well.
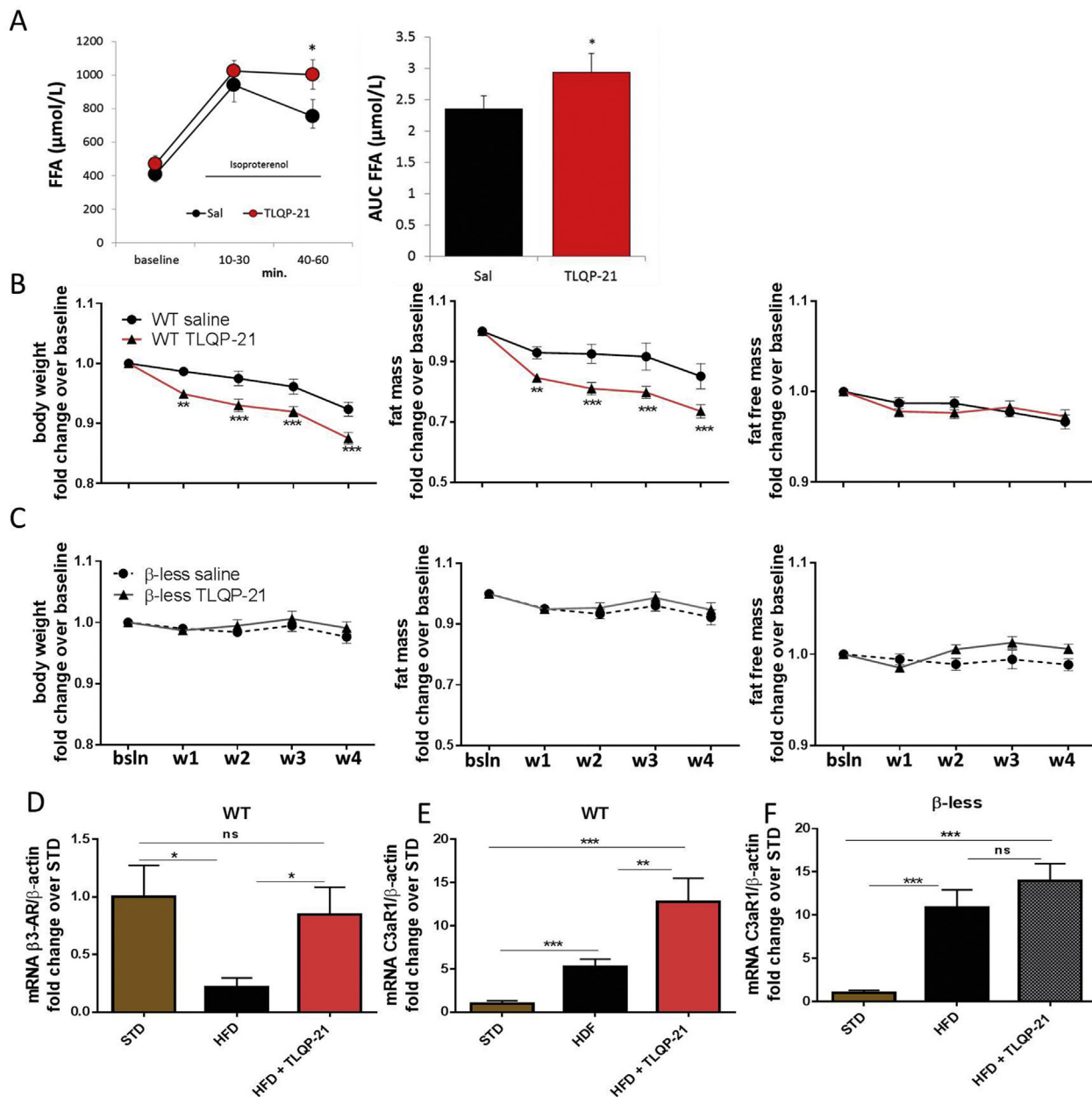
Figure 3: TLQP-21 acutely enhances ISO-induced lipolysis and chronically opposes obesity in WT but not β-less mice. (**A**) TLQP-21 (40 μg i.v.) acutely prolongs ISO-induced increase of circulating free fatty acids (FFA) in rats (n = 8 for each group) [F (2,18) = 2.7, p = 0.09]. (**B−C**) TLQP-21 (5 mg/kg/d i.p.) reduces body weight [F (1,90) = 36.89, p < 0.0001] and fat mass [F (1,90) = 24.79, p < 0.0001], but not fat free mass in diet-induced obese wild type (WT) but not β-less mice (WT saline: n = 11; TLQP-21: n = 9; β-less saline: n = 12; TLQP-21: n = 11). (**D−F**) Relative gene expression in perigonadal white adipose tissue (pWAT) of WT and β-less mice fed standard diet (STD), saline associated with high fat diet (HFD), or TLQP-21 associated with HFD (TLQP-21, HFD) (β$_3$-AR in WT, F (2,20) = 3.761, p = .043; C3aR1 in WT, F (2,20) = 13.18, p = .0002; C3aR1 in β-less, F (2,18) = 13.30, p = .0003), (N = 6−7 per group). Data represent the mean +/− SEM. *p < 0.05 **p < 0.01 ***p < 0.001.

3.4. Mechanism of TLQP-21-induced anti-obesity effect in mice

The *in vitro* and *in vivo* lipolytic effect exerted by TLQP-21 prompted us to test whether chronic TLQP-21 treatment would exert an anti-obesity effect by a mechanism requiring βARs and C3aR1. Diet-induced obese WT and β-less mice were injected daily with TLQP-21 (5 mg/kg i.p.) or saline for 4 consecutive weeks. After the first week of TLQP-21 treatment, WT mice displayed a significant decrease in body weight compared to controls; this difference was maintained over the course of 28 days of treatment (Figure 3B; Table S2). A significant decrease in fat mass in WT TLQP-21-treated mice was observed and no change in

fat-free mass (Figure 3B) and food intake (Figure S2A) were detected. Conversely, β-less mice receiving the same chronic TLQP-21 treatment displayed no reduction in body weight, food intake, fat or fat-free mass compared to saline-treated controls (Figure 3C).

It has previously been proposed that TLQP-21 activates a feed-forward pro-lipolytic mechanism [13] potentially capable of reversing obesity-associated lipolytic catecholamine resistance [5]. Chronic TLQP-21 treatment normalized high fat diet-induced downregulation of β3AR while further up-regulating the obesity-induced increased of C3aR1 mRNA [13,20] in the pWAT of WT but not of β-less mice (Figure 3D-F).

Interestingly, C3aR1 expression was indistinguishable between WT and β-less mice fed STD (WT = 0.023 ± 0.007, β-less = 0.014 ± 0.004 C3aR1/β-actin), while it was upregulated by HFD more in β-less than in WT mice (Figure 3F), further supporting the requirement of concomitant β-AR and C3aR1 signaling for TLQP-21 anti-obesity effect. Additionally, in line with the TLQP-21 anti-obesity effect, the expression of some molecular markers of mitochondrial function and thermogenesis were increased in scWAT of WT but not β-less mice (Figure S2G,H).

Based on these results and on the acute effect exerted by TLQP-21 on lipolysis (Figure 3A), we performed a MRI-based lipidomic profiling of plasma from WT mice chronically treated with TLQP-21 under fed and fasted conditions. Consistent with the mild, acute pro-lipolytic effect, TLQP-21-treated WT mice showed a mild, but not statistically significant, increase of plasma FFA (Figure S2D) without any change in the other lipid species measured (Table S3). These results prompted us to determine if there was an associated change in energy expenditure. Somewhat surprisingly, chronic peripheral TLQP-21 treatment was not associated with increased energy expenditure measured with indirect calorimetry during the fourth week of treatment in either WT and β-less mice (Figure S2A,B), a finding that was confirmed in follow-up sub-chronic treatment experiments (Figure S3). This result is at variance with the central effect of TLQP-21 infusion on energy expenditure [12], thus providing additional evidence that the central and peripheral anti-obesity mechanisms of the peptide are distinct [12,13,42,43].

Next we examined whether the TLQP-21 induced mild, pro-lipolytic and anti-obesity effects were associated with altered glucose metabolism or ectopic fat deposition. In spite of reduced body weight and adiposity, fasting glycemia and glucose tolerance were not significantly improved by chronic TLQP-21 treatment in WT mice (Figure S2C). Importantly, TLQP-21 did not increase liver or quadriceps muscle fat content (Figure S2E,F), thus excluding that mild lipolysis would cause ectopic fat accumulation and associated lypotoxicity [44]. Overall, the concomitant TLQP-21-induced moderate increase in circulating FFA and glucose-stimulated insulin secretion [17,35] might compensate each other and result in no net change in glucose homeostasis.

Finally, we investigated the selectivity and specificity of the anti-obesity effect induced by TLQP-21/C3aR1. WT obese mice were treated with the R21A peptide, an inactive mutant of TLQP-21 in which the C-terminal Arginine_{21} is mutated to Alanine_{21} [14]. As opposed to TLQP-21, the R21A peptide treatment had no effect on body weight, body composition, food intake, or energy expenditure (Figure 4A–D). Additionally, we injected HFD fed C3aR1 KO mice with saline or TLQP-21 using the same protocol previously described. TLQP-21 exerted no metabolic effect on C3aR1 KO mice (Figure 4E–H). Taken together the results obtained with the inactive R21A mutant and the C3aR1 KO mice indicate that TLQP-21 activation of C3aR1 is necessary and sufficient to explain its anti-obesity effect.

4. DISCUSSION

The development of anti-obesity drugs, which target adipocyte lipolysis has been thus far hindered by the occurrence of insulin resistance, lipotoxicity, and cardiovascular side effects [8,10]. This study identified a novel pathway of controlled lipolysis mediated by the TLQP-21 peptide and the C3aR1 receptor that opposes obesity in absence of cardiovascular or metabolic side effects [13,18, present study]. We showed that TLQP-21 does not possess lipolytic properties per se. Rather, it enhances βAR-induced lipolysis in adipocytes via $[Ca^{2+}]_i$ mobilization and MAPK/ERK activation of HSL. Furthermore, we demonstrated that chronic peripheral TLQP-21 treatment exerts an

anti-obesity effect in diet-induced obese mice requiring functional βAR and C3aR1 expression. The magnitude of TLQP-21-induced anti-obesity effect is relatively modest, yet robust, selective, and largely safe, overall paving the way for the development of more potent and stable analogues based on its mechanism of action.

The more potent and best characterized lipolytic pathways elicit Gs-mediated increase in cAMP/PKA or cGMP/PKG signaling resulting in a robust release of FFA, which is often associated with adverse effects [8]. Activation of the TLQP-21/C3aR1 pathway significantly differs from the effects exerted by these potent lipolytic molecules. Firstly, it does not elicit lipolysis per se, but it only potentiates lipolysis in the presence of β-adrenergic receptor activation, which is the primary endogenous regulator of lipolysis. Consistently, its infusion does not result in a robust elevation of FFA in vivo, thus limiting the risk for side effects. Finally, it does not increase energy expenditure, blood pressure, or insulin resistance; rather, it normalizes obesity-associated hypertension and potentiates glucose-stimulated insulin secretion [13,17,18, present study]. Pharmacological treatment with TLQP-21 reversed obesity-induced downregulation of adipose βAR expression, suggesting that activating this pathway in obesity might reverse the lipolytic catecholamine resistance usually associated with obesity [5]. The mechanism(s) responsible for the loss of fat mass in absence of increased energy expenditure or increased plasma/tissue lipids exerted by TLQP-21 are presently unknown. A similar decrease in fat mass in absence of a detectable increase in energy expenditure or decrease in food intake has previously been reported in humans and animal models testing different bioactive molecules [45,46]. Similar to these studies, TLQP-21 could promote local, rather than systemic, chronic low-grade energy expenditure [45] or futile cycles [47] that are difficult to detect with whole body indirect calorimetry. Acute or sub-chronic peripheral TLQP-21 does not increase thermogenesis, suggesting that the brown adipose tissue (BAT) is not its main target organ [13]. An alternative hypothesis is that TLQP-21 could concomitantly alter nutrient absorption from the gastro-intestinal tract [48,49].

One explanation for the apparent safe pharmacological profile exerted by TLQP-21 is its mechanism of action. C3aR1 is considered a Gi/o-coupled receptor [14,15,27], which, as we demonstrated, activates a calcium mediated signaling in adipocytes, which is unable to elicit lipolysis in absence of concomitant Gs/AC activation. We were unable to detect TLQP-21 induced increase in $[Ca^{2+}]_i$, using FURA-AM, a finding, which is consistent with lack of PLC/PKC phosphorylation induced by TLQP-21 in adipocytes [13]. Conversely, our results are compatible with C3aR1 being coupled to a Ca^{2+} channel, such as a TRP channel [50,51], eliciting a transient Ca^{2+} influx from the extra-cellular compartment as previously shown in neutrophils [32], which is difficult to detect in adipocytes due to their limited cytoplasmic compartment. Furthermore, TLQP-21 has a lower potency in activating the C3aR1 compared to C3a [14,15] while being more potent in eliciting lipolysis than C3a_{70-77} (which is ∼10 times less potent compared to C3a [26,52]). Overall TLQP-21 appears to be an ideal target to develop C3aR1 agonists for obesity related conditions.

While the role of C3aR1 in the innate immune response is well established, this receptor is now emerging with a much broader pattern of tissue expression as well as biological activity than was previously recognized [15,20,53,54]. Before TLQP-21 was identified as an endogenous ligand of C3aR1, limited work had been conducted on the role of this receptor on adipocyte function and metabolism [15,20,55]. Knockout studies targeting C3, C3aR1, and VGF suggest direct involvement of this pathway in adiposity and energy balance [20,56–60] while also highlighting the occurrence of uncharacterized compensatory effects leading to paradoxical overlapping phenotypes in
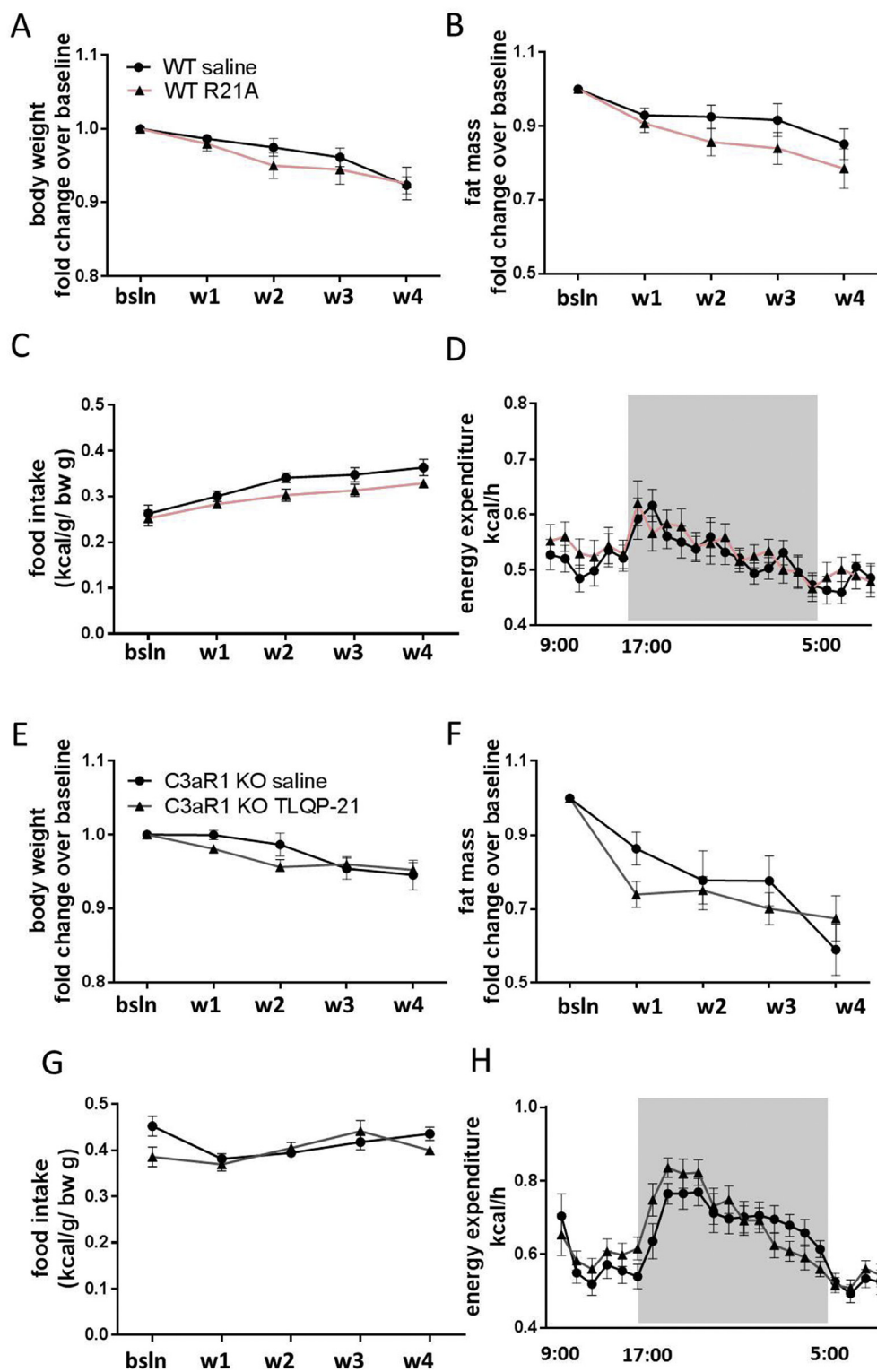
Figure 4: TLQP-21 activation of C3aR1 is necessary and sufficient for TLQP-21 anti-obesity effect. Chronic R21A peptide (5 mg/kg/d i.p.), an inactive mutant of TLQP-21, does not alter body weight (**A**), fat mass (**B**), food intake, (**C**) and energy expenditure (**D**) in WT mice fed HFD (WT HFD saline: n = 11; WT HFD R21A: n = 6). Chronic TLQP-21 (5 mg/kg/d i.p.) treatment does not affect body weight (**E**), fat mass (**F**), food intake, (**G**) and energy expenditure (**H**) in C3aR1 KO mice fed HFD (HFD saline: n = 6; C3aR1 KO HFD TLQP-21: n = 7). Data represent the mean ± SEM.

Original Article

ligands and receptor knockout strains. In obesity, a significant increase in adipose tissue C3aR1 expression has been found [20; present study], which is paralleled by a concomitant increase of TLQP-21 binding affinity to adipocyte membranes [13]. C3a, the first identified ligand for the C3aR1, is an anaphylatoxin molecule generated by the cleavage of C3 by C3 convertases [54,61–63]. Importantly, serum carboxypeptidase rapidly regulates the activity of C3a by cleaving off C-terminal arginine residue (R77) generating a des-arginine peptide (also called acylation stimulated protein, ASP) [60,64], which is inactive at C3aR1 and has been associated with triglyceride synthesis [65]. Similar to C3a, TLQP-21 residues necessary for receptor activation are located at the C-terminus. By mutating Arginine$_{21}$ into Alanine$_{21}$ (R21A peptide) in the TLQP-21 sequence we generated an inactive peptide [14; present study] that preserves its ability to bind to C3aR1 forming an α-helix [14]. A putative TLQP-21-des arginine peptide has not been identified thus far [12].

TLQP-21 is present in secretory vesicles in sympathetic nerve terminals where it co-localizes with tyrosine hydroxylase (TH), the rate limiting enzyme responsible for the biosynthesis of NE [13]. Overall, available data support a model in which TLQP-21 and NE are co-secreted and the peptide activates a C3aR1/Calcium/ERK-mediated up-regulation of NE-induced HSL activation and lipolysis. C3a derived from the circulation or adipocyte secretion and cleavage of C3 can also exert a similar effect although this remains to be characterized in light of the ASP-mediated increase in triglyceride synthesis [65]. Interestingly, the TLQP-21 effect on lipolysis is opposite to NPY-induced inhibition of adrenergic receptor-induced lipolysis [66]. Similar to TLQP-21, NPY also localizes at the sympathetic nerve terminals with TH [67]. These results suggest a complex regulation of sympathetically-secreted neurotransmitters and neuropeptides (NPY, TLQP-21) modulating lipolysis that can be targeted to finely tune lipolysis for therapeutic uses.

In conclusion, our study significantly advances the mechanistic understanding of lipolysis by identifying an alternative calcium-regulated pathway mediated by TLQP-21 and C3aR1. The mechanism that we identified could be targeted to safely treat obesity and reverse catecholamine resistance bypassing the side effects associated with the use of Gs-coupled receptor agonists and other potent pro-lipolytic mechanisms, which often lead to the development of insulin resistance and other metabolic diseases.

AUTHOR CONTRIBUTIONS

CC, MR, RH, BSS, JP, ZKG, and NAZ conducted experiment and analyzed data; CC, JMM, SMO and AB conceptualized the experiments; AB conceptualized the study design; CC and AB wrote the manuscript with the input from co-authors.

ACKNOWLEDGMENTS

CONFLICT OF INTEREST

None declared.

APPENDIX A. SUPPLEMENTARY DATA

Supplementary data related to this article can be found at http://dx.doi.org/10.1016/j.molmet.2016.10.005.

REFERENCES

[1] Schwartz, M.W., Woods, S.C., Porte Jr., D., Seeley, R.J., Baskin, D.G., 2000. Central nervous system control of food intake. Nature 404(6778):661–671.

[2] Lowell, B.B., Spiegelman, B.M., 2000. Towards a molecular understanding of adaptive thermogenesis. Nature 404(6778):652–660.

[3] Guh, D.P., Zhang, W., Bansback, N., Amarsi, Z., Birmingham, C.L., Anis, A.H., 2009. The incidence of co-morbidities related to obesity and overweight: a systematic review and meta-analysis. BMC Public Health 25:9–88.

[4] Kopelman, P.G., 2000. Obesity as a medical problem. Nature 404(6778):635–643.

[5] Lönnqvist, F., Wahrenberg, H., Hellström, L., Reynisdottir, S., Arner, P., 1992. Lipolytic catecholamine resistance due to decreased beta 2-adrenoceptor expression in fat cells. Journal of Clinical Investigation 90(60):2175–2186.

[6] Large, V., Reynisdottir, S., Langin, D., Fredby, K., Klannemark, M., Holm, C., et al., 1999. Decreased expression and function of adipocyte hormone-sensitive lipase in subcutaneous fat cells of obese subjects. Journal of Lipid Research 40(11):2059–2066.

[7] Mowers, J., Uhm, M., Reilly, S.M., Simon, J., Leto, D., Chiang, S.H., et al., 2013. Inflammation produces catecholamine resistance in obesity via activation of PDE3B by the protein kinases IKKε and TBK1. Elife 2:e01119.

[8] Arner, P., Langin, D., 2014. Lipolysis in lipid turnover, cancer cachexia, and obesity-induced insulin resistance. Trends in Endocrinology & Metabolism 25(5):255–262.

[9] Coleman, R.A., Mashek, D.G., 2011. Mammalian triacylglycerol metabolism: synthesis, lipolysis, and signaling. Chemical Reviews 111(10):6359–6386.

[10] Morigny, P., Houssier, M., Mouisel, E., Langin, D., 2016. Adipocyte lipolysis and insulin resistance. Biochimie 125:259–266.

[11] Mottillo, E.P., Shen, X.J., Granneman, J.G., 2007. Role of hormone-sensitive lipase in beta-adrenergic remodeling of white adipose tissue. American Journal of Physiology — Endocrinology and Metabolism 293(5):E1188–E1197.

[12] Bartolomucci, A., La Corte, G., Possenti, R., Locatelli, V., Rigamonti, A.E., Torsello, A., et al., 2006. TLQP-21, a VGF-derived peptide, increases energy expenditure and prevents the early phase of diet-induced obesity. Proceedings of the National Academy of Sciences of the United States of America 103(39):14584–14594.

[13] Possenti, R., Muccioli, G., Petrocchi, P., Cero, C., Cabassi, A., Vulchanova, L., et al., 2012. Characterization of a novel peripheral pro-lipolytic mechanism in mice: role of VGF-derived peptide TLQP-21. Biochemical Journal 441:511–522.

[14] Cero, C., Vostrikov, V.V., Verardi, R., Severini, C., Gopinath, T., Braun, P.D., et al., 2014. The TLQP-21 peptide activates the G-protein-coupled receptor C3aR1 via a folding-upon-binding mechanism. Structure 22(12):1744–1753.

[15] Hannedouche, S., Beck, V., Leighton-Davies, J., Beibel, M., Roma, G., Oakeley, E.J., et al., 2013. Identification of the C3a receptor (C3AR1) as the target of the VGF-derived peptide TLQP-21 in rodent cells. Journal of Biological Chemistry 288(38):27434–27443.

[16] Fairbanks, C.A., Peterson, C.D., Speltz, R.H., Riedl, M.S., Kitto, K.F., Dykstra, J.A., et al., 2014. The VGF-derived peptide TLQP-21 contributes to inflammatory and nerve injury-induced hypersensitivity. Pain 155(7):1229–1237.

[17] Stephens, S.B., Schisler, J.C., Hohmeier, H.E., An, J., Sun, A.Y., Pitt, G.S., et al., 2012. A VGF-derived peptide attenuates development of type 2 diabetes via enhancement of islet β-cell survival and function. Cell Metabolism 16:33–43.

[18] Fargali, S., Garcia, A.L., Sadahiro, M., Jiang, C., Janssen, W.G., Lin, W.J., et al., 2014. The granin VGF promotes genesis of secretory vesicles, and regulates circulating catecholamine levels and blood pressure. FASEB Journal 28(5): 2120—2133.

[19] D'Amato, F., Noli, B., Angioni, L., Cossu, E., Incani, M., Messana, I., et al., 2015. VGF peptide profiles in type 2 diabetic patients' plasma and in obese mice. PLoS One 10(11):e0142333.

[20] Mamane, Y., Chung Chan, C., Lavallee, G., Morin, N., Xu, L.J., Huang, J., et al., 2009. The C3a anaphylatoxin receptor is a key mediator of insulin resistance and functions by modulating adipose tissue macrophage infiltration and activation. Diabetes 58(9):2006—2017.

[21] Bachman, E.S., Dhillon, H., Zhang, C.Y., Cinti, S., Bianco, A.C., Kobilka, B.K., et al., 2002. betaAR signaling required for diet-induced thermogenesis and obesity resistance. Science 297(5582):843—845.

[22] Tschöp, M.H., Speakman, J.R., Arch, J.R., Auwerx, J., Brüning, J.C., Chan, L., et al., 2011. A guide to analysis of mouse energy metabolism. Nature Methods 9: 57—63.

[23] Razzoli, M., Frontini, A., Gurney, A., Mondini, E., Cubuk, C., Katz, L.S., et al., 2015 Nov 11. Stress-induced activation of brown adipose tissue prevents obesity in conditions of low adaptive thermogenesis. Molecular Metabolism 5(1):19—33.

[24] Pollesello, P., Masutti, F., Crocè, L.S., Toffanin, R., Eriksson, O., Paoletti, S., et al., 1993. 1H NMR spectroscopic studies of lipid extracts from human fatty liver. Biochemical and Biophysical Research Communications 14:1217—1222.

[25] Sparling, M.L., Zidovetzki, R., Muller, L., Chan, S.I., 1989. Analysis of membrane lipids by 500 MHz 1H NMR. Analytical Biochemistry 178:67—76.

[26] Hugli, T.E., Erickson, B.W., 1977. Synthetic peptides with the biological activities and specificity of human C3a anaphylatoxin. Proceedings of the National Academy of Sciences of the United States of America 74(5):1826—1830.

[27] Klos, A., Wende, E., Wareham, K.J., Monk, P.N., 2013. Complement peptide C5a, C4a, and C3a receptors. Pharmacological Reviews 65(1):500—543.

[28] Litosch, I., Hudson, T.H., Mills, I., Li, S.Y., Fain, J.N., 1982. Forskolin as an activator of cyclic AMP accumulation and lipolysis in rat adipocytes. Molecular Pharmacology 22(1):109—115.

[29] Schimmel, R.J., 1984. Stimulation of cAMP accumulation and lipolysis in hamster adipocytes with forskolin. American Journal of Physiology 246(1 Pt 1): C63—C68.

[30] Tavernier, G., Jimenez, M., Giacobino, J.P., Hulo, N., Lafontan, M., Muzzin, P., et al., 2005. Norepinephrine induces lipolysis in beta1/beta2/beta3-adrenoceptor knockout mice. Molecular Pharmacology 68(3):793—799.

[31] Chen, Y.C., Pristerá, A., Ayub, M., Swanwick, R.S., Karu, K., Hamada, Y., et al., 2013. Identification of a receptor for neuropeptide VGF and its role in neuropathic pain. Journal of Biological Chemistry 288(48):34638—34646.

[32] Norgauer, J., Dobos, G., Kownatzki, E., Dahinden, C., Burger, R., Kupper, R., et al., 1993. Complement fragment C3a stimulates Ca2+ influx in neutrophils via a pertussis-toxin-sensitive G protein. European Journal of Biochemistry 217(1): 289—294.

[33] Severini, C., Ciotti, M.T., Biondini, L., Quaresima, S., Rinaldi, A.M., Levi, A., et al., 2008. TLQP-21, a neuroendocrine VGF-derived peptide, prevents cerebellar granule cells death induced by serum and potassium deprivation. Journal of Neurochemistry 104(2):534—544.

[34] Petrocchi-Passeri, P., Biondini, L., Mongiardi, M.P., Mordini, N., Quaresima, S., Frank, C., et al., 2013. Neuropeptide TLQP-21, a VGF internal fragment, modulates hormonal gene expression and secretion in GH3 cell line. Neuroendocrinology 97(3):212—224.

[35] Petrocchi-Passeri, P., Cero, C., Cutarelli, A., Frank, C., Severini, C., Bartolomucci, A., et al., 2015. The VGF-derived peptide TLQP-62 modulates insulin secretion and glucose homeostasis. Journal of Molecular Endocrinology 54(3):227—239.

[36] Agell, N., Bachs, O., Rocamora, N., Villalonga, P., 2002. Modulation of the Ras/Raf/MEK/ERK pathway by Ca(2+), and calmodulin. Cell Signal 14(8):649—654.

[37] Cullen, P.J., Lockyer, P.J., 2002. Integration of calcium and Ras signaling. Nature Reviews Molecular Cell Biology 3(5):339—348.

[38] Chuderland, D., Seger, R., 2008. Calcium regulates ERK signaling by modulating its protein—protein interactions. Communicative & Integrative Biology 1(1):4—5.

[39] Greenberg, A.S., Shen, W.J., Muliro, K., Patel, S., Souza, S.C., Roth, R.A., et al., 2001. Stimulation of lipolysis and hormone-sensitive lipase via the extracellular signal-regulated kinase pathway. Journal of Biological Chemistry 276(48):45456—45461.

[40] Arner, P., Kriegholm, E., Engfeldt, P., 1991. In vivo interactions between beta-1 and beta-2 adrenoceptors regulate catecholamine tachyphylaxia in human adipose tissue. Journal of Pharmacology and Experimental Therapeutics 259(1):317—322.

[41] Guo, Z., Johnson, C.M., Jensen, M.D., 1997. Regional lipolytic responses to isoproterenol in women. American Journal of Physiology 273(1 Pt 1):E108—E112.

[42] Foglesong, G.D., Huang, W., Liu, X., Slater, A.M., Siu, J., Yildiz, V., et al., 2016. Role of hypothalamic VGF in energy balance and metabolic adaption to environmental enrichment in mice. Endocrinology 157(3):983—996.

[43] Sadahiro, M., Erickson, C., Lin, W.J., Shin, A.C., Razzoli, M., Jiang, C., et al., 2015. Role of VGF-derived carboxy-terminal peptides in energy balance and reproduction: analysis of "humanized" knockin mice expressing full-length or truncated VGF. Endocrinology 156(5):1724—1738.

[44] Virtue, S., Vidal-Puig, A., 2010. Adipose tissue expandability, lipotoxicity and the Metabolic Syndrome—an allostatic perspective. Biochimica Biophysica Acta 1801(3):338—349.

[45] Bal, N.C., Maurya, S.K., Sopariwala, D.H., Sahoo, S.K., Gupta, S.C., Shaikh, S.A., et al., 2012. Sarcolipin is a newly identified regulator of muscle-based thermogenesis in mammals. Nature Medicine 18(10):1575—1579.

[46] Yoneshiro, T., Aita, S., Matsushita, M., Kayahara, T., Kameya, T., Kawai, Y., et al., 2013. Recruited brown adipose tissue as an antiobesity agent in humans. Journal of Clinical Investigation 123(8):3404—3408.

[47] Kazak, L., Chouchani, E.T., Jedrychowski, M.P., Erickson, B.K., Shinoda, K., Cohen, P., et al., 2015. A creatine-driven substrate cycle enhances energy expenditure and thermogenesis in beige fat. Cell 163(3):643—655.

[48] Severini, C., La Corte, G., Improta, G., Broccardo, M., Agostini, S., Petrella, C., et al., 2009. In vitro and in vivo pharmacological role of TLQP-21, a VGF-derived peptide, in the regulation of rat gastric motor functions. British Journal of Pharmacology 157(6):984—993.

[49] Petrella, C., Broccardo, M., Possenti, R., Severini, S., Improta, G., 2012. TLQP-21, a VGF-derived peptide, stimulates exocrine pancreatic secretion in the rat. Peptides 36(1):133—136.

[50] Damann, N., Voets, T., Nilius, B., 2008. TRPs in our senses. Current Biology 18(18):R880—R889.

[51] Sukumar, P., Sedo, A., Li, J., Wilson, L.A., O'Regan, D., Lippiat, J.D., et al., 2012. Constitutively active TRPC channels of adipocytes confer a mechanism for sensing dietary fatty acids and regulating adiponectin. Circulation Research 111(2):191—200.

[52] Ember, J.A., Johansen, N.L., Hugli, T.E., 1991. Designing synthetic super-agonists of C3a anaphylatoxin. Biochemistry 30(15):3603—3612.

[53] Coulthard, L.G., Woodruff, T.M., 2015. Is the complement activation product C3a a proinflammatory molecule? Re-evaluating the evidence and the myth. Journal of Immunology 194(8):3542—3548.

[54] Lo, J.C., Ljubicic, S., Leibiger, B., Kern, M., Leibiger, I.B., Moede, T., et al., 2014. Adipsin is an adipokine that improves β cell function in diabetes. Cell 158(1):41—53.

[55] Lim, J., Iyer, A., Suen, J.Y., Seow, V., Reid, R.C., Brown, L., et al., 2013. C5aR and C3aR antagonists each inhibit diet-induced obesity, metabolic dysfunction, and adipocyte and macrophage signaling. FASEB Journal 27(2):822—831.

[56] Hahm, S., Fekete, C., Mizuno, T.M., Windsor, J., Yan, H., Boozer, C.N., et al., 2002. VGF is required for obesity induced by diet, gold thioglucose treatment, and agouti and is differentially regulated in pro-opiomelanocortin- and neuropeptide Y-containing arcuate neurons in response to fasting. Journal of Neuroscience 22(16):6929—6938.

Original Article

[57] Hahm, S., Mizuno, T.M., Wu, T.J., Wisor, J.P., Priest, C.A., Kozak, C.A., et al., 1999. Targeted deletion of the Vgf gene indicates that the encoded secretory peptide precursor plays a novel role in the regulation of energy balance. Neuron 23(3):537—548.

[58] Watson, E., Hahm, S., Mizuno, T.M., Windsor, J., Montgomery, C., Scherer, P.E., et al., 2005. VGF ablation blocks the development of hyperinsulinemia and hyperglycemia in several mouse models of obesity. Endocrinology 146(12):5151—5163.

[59] Roy, C., Paglialunga, S., Fisette, A., Schrauwen, P., Moonen-Kornips, E., St-Onge, J., et al., 2008. Shift in metabolic fuel in acylation-stimulating protein-deficient mice following a high-fat diet. American Journal of Physiology — Endocrinology and Metabolism 294(6):E1051—E1059.

[60] Murray, I., Havel, P.J., Sniderman, A.D., Cianflone, K., 2000. Reduced body weight, adipose tissue, and leptin levels despite increased energy intake in female mice lacking acylation-stimulating protein. Endocrinology 141(3): 1041—1049.

[61] Markiewski, M.M., Lambris, J.D., 2007. The role of complement in inflammatory diseases from behind the scenes into the spotlight. American Journal of Pathology 171(3):715—727.

[62] Nettesheim, D.G., Edalji, R.P., Mollison, K.W., Greer, J., Zuiderweg, E.R., 1988. Secondary structure of complement component C3a anaphylatoxin in solution as determined by NMR spectroscopy: differences between crystal and solution conformations. Proceedings of the National Academy of Sciences of the United States of America 85(14):5036—5040.

[63] White, R.T., Damm, D., Hancock, N., Rosen, B.S., Lowell, B.B., Usher, P., et al., 1992. Human adipsin is identical to complement factor D and is expressed at high levels in adipose tissue. Journal of Biological Chemistry 267(13):9210—9213.

[64] Cianflone, K., Xia, Z., Chen, L.Y., 2003. Critical review of acylation-stimulating protein physiology in humans and rodents. Biochimica et Biophysica Acta 1609(2):127—143.

[65] Murray, I., Köhl, J., Cianflone, K., 15 Aug 1999. Acylation-stimulating protein (ASP): structure-function determinants of cell surface binding and triacylglycerol synthetic activity. Biochemical Journal 342(Pt 1):41—48.

[66] Bradley, R.L., Mansfield, J.P., Maratos-Flier, E., 2005. Neuropeptides, including neuropeptide Y and melanocortins, mediate lipolysis in murine adipocytes. Obesity Research 13(4):653—661.

[67] Giordano, A., Frontini, A., Murano, I., Tonello, C., Marino, M.A., Carruba, M.O., et al., 2005. Regional-dependent increase of sympathetic innervation in rat white adipose tissue during prolonged fasting. Journal of Histochemistry & Cytochemistry 53(6):679—687.